

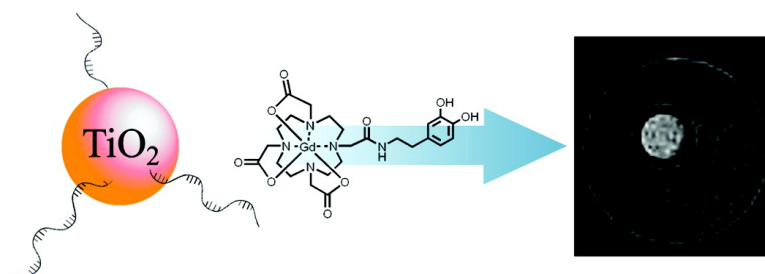
Communication

DNA–TiO Nanoconjugates Labeled with Magnetic Resonance Contrast Agents

Paul J. Endres, Tatjana Paunesku, Stefan Vogt, Thomas J. Meade, and Gayle E. Woloschak

J. Am. Chem. Soc., **2007**, 129 (51), 15760-15761 • DOI: 10.1021/ja0772389

Downloaded from <http://pubs.acs.org> on February 9, 2009



More About This Article

Additional resources and features associated with this article are available within the HTML version:

- Supporting Information
- Links to the 4 articles that cite this article, as of the time of this article download
- Access to high resolution figures
- Links to articles and content related to this article
- Copyright permission to reproduce figures and/or text from this article

[View the Full Text HTML](#)



ACS Publications
 High quality. High impact.

DNA–TiO₂ Nanoconjugates Labeled with Magnetic Resonance Contrast Agents

Paul J. Endres,[†] Tatjana Paunesku,[‡] Stefan Vogt,[§] Thomas J. Meade,^{*,†,‡} and Gayle E. Woloschak^{*,‡}

Departments of Chemistry, Biochemistry and Molecular and Cell Biology, Neurobiology and Physiology, Radiology, and Radiation Oncology, Northwestern University, 2145 Sheridan Road, Evanston, Illinois 60208, and Experimental Facilities Division, Argonne National Laboratory, 9700 South Cass Avenue, Argonne, Illinois 60439

Received September 21, 2007; E-mail: tmeade@northwestern.edu; g-woloschak@northwestern.edu

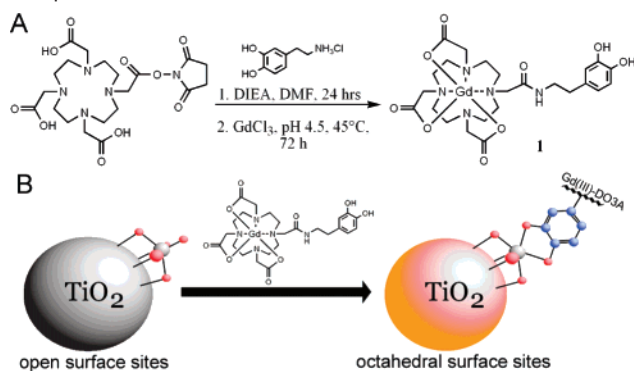
Recent efforts to develop nanoscale materials for use as biocompatible delivery scaffolds for drugs and imaging agents have produced significant advances in the area of multifunctional probes.¹ These new materials provide the means to chaperone and concentrate both drugs and contrast agents in specific organs, tissues, and cells.² Primarily, superparamagnetic (SPIO) nanoparticles, known for their ability to enhance signal contrast in *T*₂-weighted MR images, have dominated reports employing this approach.^{3,4} These agents typically result in negative contrast enhancement, and occasionally, their inherent magnetic susceptibility leads to background artifacts.³ Conversely, *T*₁ contrast agents do not suffer from this phenomenon. However, there are very few examples of paramagnetic (*T*₁)-labeled nanoparticles that combine therapeutics with an MR reporter.⁵

In conjunction, our recent work shows that TiO₂ nanoparticles decorated with DNA oligonucleotides function in a targeted and therapeutic capacity.^{6,7} Targeting is accomplished via oligonucleotide hybridization to an intracellular organelle's matching DNA sequence, and therapeutic activity is elicited by light-induced scission of the nanoparticle-bound DNA. Considering these properties, attachment of a *T*₁ contrast agent to such a targeted nanoparticle would allow the visualization of certain genomic sequences in cells and tissues via MRI. Knowing that cancer is a result of DNA mutations, one can envision that a therapeutic MR probe targeting only mutant oncogene sequences would have a significant impact on the therapeutic and diagnostic communities. As a result, we have functionalized DNA-labeled nanoconjugates with a Gd(III)-based contrast agent to produce a biocompatible, therapeutically active delivery scaffold that is detectable by routine *T*₁-weighted MR imaging.⁷

The Gd(III)-labeled nanoparticles were prepared from previously reported TiO₂–oligonucleotide nanoconjugates.^{6,7} The TiO₂ nanoparticles (3–5 nm) are surface modified by exploiting their selective reactivity to ortho-substituted enediol ligands (such as dopamine).⁸ These reactions form semiconducting, photocatalytically cleavable bonds which allow for the surface conjugation of dopamine-modified DNA. This nanoparticle-bound DNA retains its subcellular targeting capabilities while remaining stable enough to allow in vivo compartmental accumulation before photocatalytic cleavage is induced.⁷

The synthesis of a dopamine-modified contrast agent was accomplished by coupling the commercially available succinimidyl ester activated 1,4,7,10-tetraazacyclododecane-1,4,7-tetraacetic acid to dopamine hydrochloride (Scheme 1). Metalation (with GdCl₃) and purification were carried out under strict pH control as the catechol in the metalated complex (**1**) is easily oxidized at pH > 5.

Scheme 1. (A) Synthetic Route to **1**; A Dopamine-Modified MR Contrast Agent (DOPA–DO3A) and (B) Functionalization of TiO₂ Nanoparticles with **1**



Following characterization (HPLC, ESI-MS, and EA), the dopamine-modified contrast agent (**1**) was reacted with TiO₂ nanoparticles in the presence and absence of surface-conjugated oligonucleotides (see Supporting Information, S6–S9). Coupling **1** to the nanoparticle was initially detected by a distinct color change resulting from a red shift in nanoparticle absorption between the unmodified nanoparticles (white) to the modified nanoparticles (orange/brown).⁸ In addition, formation of the DOPA–DO3A nanoparticles was confirmed by UV and IR spectroscopy (see Supporting Information, S10 and S11). The modified nanoparticles revealed a characteristic rise in UV light absorption toward higher energies (200–360 nm) that has been attributed to semiconducting nanocomposites.^{8,9} Similarly, the modified nanoconjugates showed significant (20% increase) IR absorption over control nanoparticles in the carbon–carbon double bond and aromatic stretching frequencies of 1540–1680 cm⁻¹.

As expected, conjugation of **1** to the DNA-modified nanoconjugates occurs in a linear relationship to the equivalents added. The success of the conjugation reaction (assessed by the ICP-MS of Ti and Gd in purified trials of varying [**1**]:[TiO₂ active site] equivalents) increases linearly until the ratio of [**1**]:[TiO₂ active sites] reaches 1.0. At a 1:1 equivalence ratio, the conjugation reaction plateaus, giving a value of 4.6 ± 0.2% of functionalized TiO₂ active sites at ratios extending to 5:1. This is most likely due to steric effects as the available TiO₂ active sites may be blocked by the DNA oligonucleotides and the freely rotating, surface-conjugated DOPA–DO3A contrast agents.¹⁰

To determine the relaxivity of the DOPA–DO3A–TiO₂ nanoconjugates, the slope of the line generated by plotting the inverse of the *T*₁ relaxation time versus Gd(III) concentration was measured (see Supporting Information, S12). The nanoconjugates yielded a relaxivity of 3.5 ± 0.1 mM⁻¹ s⁻¹ per Gd(III) ion, similar to clinical small molecule contrast agents.¹¹ On the basis of the Ti:Gd ratio acquired from ICP-MS, each individual nanoparticle has an average

[†] Departments of Chemistry, Biochemistry and Molecular and Cell Biology, Neurobiology and Physiology, Northwestern University.

[‡] Departments of Radiology and Radiation Oncology, Northwestern University.

[§] Argonne National Laboratory.

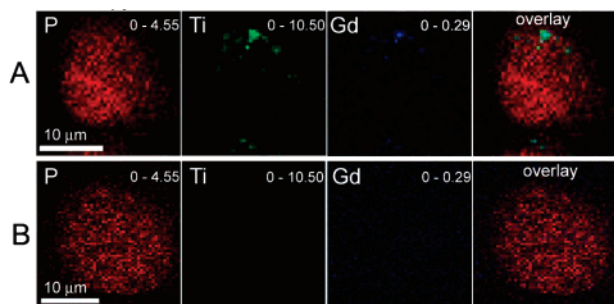


Figure 1. Two-dimensional XRF maps of (A) transfection of PC12 cells with DNA–DOPA–DO3A-modified nanoconjugates; (B) control, non-transfected PC12 cells. Phosphorus is red, titanium is green, and gadolinium is blue. The scale bars represent 10 μm . Note that each image is scaled to its respective maximum value (displayed at the upper right corner and given in $\mu\text{g}/\text{cm}^2$).



Figure 2. T_1 -weighted MR images of (A) control PC3M cells ($T_1 = 3527 \pm 48$ ms); (B) PC3M cells incubated with 0.001 mM DNA–DOPA–DO3A nanoparticles with 1.8% TiO_2 active site coverage ($T_1 = 2178 \pm 88$ ms); (C) PC3M cells incubated with 0.001 mM DNA–DOPA–DO3A nanoparticles with 4.4% TiO_2 active site coverage ($T_1 = 2356 \pm 100$ ms). The scale bar represents 0.5 mm (at 14.1 T within a FOV of 20 mm and a slice thickness of 0.5 mm). T_1 values were confirmed to be statistically different via student t tests at a 95% confidence level (Supporting Information Table S4).

relaxivity of $61.0 \pm 1.7 \text{ mM}^{-1} \text{ s}^{-1}$. In order to assess the viability of **1** to enhance the MR image contrast of the TiO_2 nanoparticles, DOPA–DO3A– TiO_2 nanoconjugates at varying [1]:[TiO_2 active site] ratios were gravity packed in glass capillary tubes and imaged. As expected, the TiO_2 nanoconjugates functionalized with **1** display a brighter signal than the control nanoparticles (see Supporting Information Figure S4).

The cellular distribution and single cell association of the DOPA–DO3A– TiO_2 nanoconjugates were evaluated by X-ray fluorescence (XRF).¹² XRF data, when deconvoluted and standardized, provides high-resolution ($0.3 \times 0.3 \mu\text{m}$), two-dimensional images that can be employed to map locations and total elemental concentrations in a desired subcellular region of interest.⁶ Therefore, this imaging modality allows direct visualization of the optically undetectable nanoconjugates while simultaneously providing cellular outlines and contrast agent location (phosphorus and gadolinium, respectively).^{12,13}

A DNA oligonucleotide targeted to the mitochondrial genome was used to functionalize the nanoparticles. The targeting sequence was specific for the sense strand of a NADH dehydrogenase 2 (ND2) mitochondrial gene present in the rat PC12 cell line: 5'-carboxy dT-cacgacaccttagcaccacacttac (ND2s).⁷ Presence of nanoconjugates in the cytoplasmic but not the nuclear regions suggests localization in either the targeted organelle, mitochondria, or possibly endosomes (this oligonucleotide has previously shown sequence specificity in this cell line).⁷ Colocalization of the Ti and Gd fluorescence signals reveals that the DOPA–DO3A– TiO_2 nanoconjugates are biologically stable and that their presence inside cells is responsible for the increase in MR image intensity versus control untreated cells (Figure 1).¹²

To assess the biocompatibility and MR image contrast of the modified nanoparticles in vitro, PC3M cells were imaged after

incubation with the nanoconjugates (Figure 2). Comparison of the images from Figure 2 reveals that the cells incubated with the DOPA–DO3A nanoconjugates display a greater contrast enhancement over control cells. Corroborating the nanoconjugate phantom images (Supporting Information Figure S4) and XRF images (Figure 1), we see that Figure 2 demonstrates the utility of quantitative T_1 analysis and XRF to predict viable contrast enhancement via MR imaging.

In conclusion, we have prepared a Gd(III)-modified DNA– TiO_2 semiconducting nanoparticle that is detectable in cells by MR imaging. The labeled particles appear to be retained at specific locations inside cells by the conjugated DNA oligonucleotides hybridizing to intracellular targets, hence creating the first nanoparticle system capable of targeting specific DNA sequences while being simultaneously detected by MR imaging.⁷ As a result, we anticipate that any dopamine-functionalized molecule (e.g., cell-penetrating peptides for passive cell membrane transport) can be linked to this modified TiO_2 nanoparticle scaffold, allowing noninvasive monitoring of cells containing target molecules and removal of target gene sequences pending TiO_2 excitation.

Acknowledgment. We thank Keith W. MacRenaris for helpful discussions, P. N. Venkatasubramanian at the Center for Basic MR Research (CBMRR) for assistance with MR image acquisition, and Drs. Aiguo Wu, Mohammed Aslam, and Vinayak Dravid for assistance and materials concerning nanoparticle synthesis. This research was supported by the National Institutes of Health under Grant Numbers 1 R01 EB005866-01 and R01 EB0021000, and the National Cancer Institute under Grant Numbers 5 U54 CA90810 and R01 CA107467. Use of the Advanced Photon Source was supported by the U.S. Department of Energy, Office of Science, Office of Basic Energy Sciences, under Contract Number W-31-109-ENG-38. The MR images were acquired on a 14.1 T-WB imaging spectrometer operated by the CBMRR under NIH/NCRR Grant Number 1 S10 RR13880-01.

Supporting Information Available: Experimental details. This material is available free of charge via the Internet at <http://pubs.acs.org>.

References

- (1) (a) Horak, D.; et al. *Bioconjugate Chem.* **2007**, *18* (3), 635–644. (b) Tkachenko, A. G.; et al. *Bioconjugate Chem.* **2004**, *15* (3), 482–490. (c) Xu, X.-H. N.; et al. *Biochemistry* **2004**, *43* (32), 10400–10413. (d) Zhang, Y.; et al. *Nano Lett.* **2006**, *6* (9), 1988–1992. (e) Bull, S. R.; et al. *Nano Lett.* **2005**, *5* (1), 1–4.
- (2) (a) Caruthers, S. D.; et al. *Curr. Opin. Biotechnol.* **2007**, *18* (1), 26–30. (b) Maysinger, D. *Org. Biomol. Chem.* **2007**, *5* (15), 2335–2342.
- (3) Bulte, J. W. M.; Kraitchman, D. L. *NMR Biomed.* **2004**, *17* (7), 484–499.
- (4) (a) Dobson, J. *Drug Dev. Res.* **2006**, *67* (1), 55–60. (b) Lind, K.; et al. *J. Drug Target* **2002**, *10* (3), 221–230. (c) Nitin, N.; et al. *J. Biol. Inorg. Chem.* **2004**, *9* (6), 706–712. (d) Zhao, M.; et al. *Bioconjugate Chem.* **2002**, *13* (4), 840–844. (e) Atanasijevic, T.; et al. *Proc. Natl. Acad. Sci. U.S.A.* **2006**, *103* (40), 14707–14712. (f) Hong, J.; et al. *Nanotechnology* **2007**, *18* (13), 135608/1–135608/6. (g) Na, H. B.; et al. *Angew. Chem., Int. Ed.* **2007**, *46* (28), 5397–5401. (h) Neuberger, T.; et al. *J. Magn. Mater.* **2005**, *293* (1), 483–496. (i) Frullano, L.; Meade, T. J. *J. Biol. Inorg. Chem.* **2007**, *12* (7), 939–949.
- (5) (a) Voisin, P.; et al. *Bioconjugate Chem.* **2007**, *18* (4), 1053–1063. (b) Guccione, S.; et al. *Methods Enzymol.* **2004**, *386* (Imaging in Biological Research, Part B), 219–236.
- (6) Paunesku, T.; et al. *Nat. Mater.* **2003**, *2* (5), 343–346.
- (7) Paunesku, T.; et al. *Nano Lett.* **2007**, *7* (3), 596–601.
- (8) Rajh, T.; et al. *J. Phys. Chem. B* **2002**, *106* (41), 10543–10552.
- (9) Rajh, T.; et al. *J. Phys. Chem. B* **1999**, *103* (18), 3515–3519.
- (10) Toth, E.; et al. *Top. Curr. Chem.* **2002**, *221* (Contrast Agents I), 61–101.
- (11) Caravan, P.; et al. *Chem. Rev.* **1999**, *99* (9), 2293–2352.
- (12) Endres, P. J.; et al. *Mol. Imaging* **2006**, *5* (4), 485–497.
- (13) Twining, B.; et al. *Anal. Chem.* **2003**, *75* (15), 3806–3816.

JA0772389